Journal of Applied Polymer Science

Nonmonotonic piezoresistive effect in elastomeric composite films

M. Paliy,[1,2] T. Trebicky,[1,2] Q. Guo,[1] B. Kobe,[2] N. Suhan,[3] G. Arsenault,[3] L. Ferrari,[3] J. Yang[1]

[1]Mechanical and Materials Engineering, Western University, London Ontario, Canada N6A 5B9

[2]Surface Science Western, Western University, London Ontario, Canada N6A 5B9

[3]Lanxess, Inc., London Ontario, Canada N6G 4X8

Correspondence to: J. Yang (E-mail: jyang@eng.uwo.ca)

ABSTRACT: We compared the change of electrical resistance with elongation (piezoresistive effect) in thin films made of conductive multiwalled carbon nanotubes embedded in eight different elastomers. Two distinct forms of piezoresistive effect were observed: (i) in the "monotonic" (M) case, the film resistance always increased with the applied strain; (ii) the "nonmonotonic" (NM) case showed an initial increase in the resistance, while with further elongation the resistance began to decrease. By varying the amount of nitrile and/or styrene groups in the polymer matrix one can alter the piezoresistive effect qualitatively: composites with ~25 wt % or more of nitrile or styrene functional side groups exhibited M piezoresistance, while others, with no, or methyl side groups only, showed NM piezoresistance. Influence of the second filler (either conductive carbon black or nonconductive nanoclay) in the ternary composites on the piezoresistive effect was explored. The possibility to modify the piezoresistive behavior of the conductive elastomer composites, for example, via chemical modification of the polymeric matrix, opens up a new venue for practical applications such as diverse types of sensors and, in NM case, complex dynamical systems (bistable elements, electromechanical oscillators, etc.) in the MEMS field. © 2016 Wiley Periodicals, Inc. J. Appl. Polym. Sci. **2016**, *133*, 43518.

KEYWORDS: composites; conducting polymers; elastomers; graphene and fullerenes; nanotubes; surfaces and interfaces

Received 7 July 2015; accepted 4 February 2016

DOI: 10.1002/app.43518

INTRODUCTION

The piezoresistive effect is the change of electrically conductive properties of a material under an applied stress/strain. Piezoresistive effect is trivial in metals, where bulk resistivity $\rho = \rho_0$ stays constant during deformation, while the resistance R of a sample changes monotonically merely due to change in its geometry. For example, for a metal wire under uniaxial stretching, resistance R grows with strain ε as $R = \rho^{L}/_{A} = R_0(1+\varepsilon)^{1+2v}$, where R_0 is initial resistance, L is its length, A is its cross-sectional area, and v is the Poisson's ratio. Semiconductors may exhibit more complex behavior with deformation, where the bulk resistivity ρ depends on stress/strain,[1] for example, it can decrease with strain (negative piezoresistivity[2]).

A rich variety of piezoresistive behaviors are observed in novel conductive and stretchable composite materials. Such materials typically consist of an insulating elastomer matrix and one or more conductive nanoparticulate filler, such as carbon black (CB), carbon nanotubes (CNTs), metal nanoparticles or nanowires.[3–5] The change of the electromechanical properties of an individual CNT with applied stress has been extensively studied both theoretically and experimentally.[6–9] However, what matters in the composites is the morphology of the conductive network formed by the filler particles.[3,5] In a typical case, both bulk resistance (or sheet resistance in the case of a film) and bulk resistivity increase monotonically with elongation.[10,11] Such composite materials are often used as deformation/pressure sensors,[12–14] especially if their resistance change is steep. In contrast, for stretchable conductive wires, one seeks materials that maintain constant resistance as a function of stretching.[15] Moreover, complex phenomena as hysteresis, history dependence, relaxation, or temporal dependence of resistance can be observed in composite conductive materials.[4,15,16]

A few papers report an intriguing nonmonotonic (NM) change of the conductive properties of the composite samples with elongation.[16–24] Typically, after an initial growth, the resistivity begins to decrease with further elongation. This NM behavior has been qualitatively known for several decades[25] in certain rubber composites with carbon or metallic filler particulates, but a sound explanation and clarification of it is still needed. General hypothesis of competition between the processes of breaking the existing conducting paths and the formation of the new conducting paths upon stretching is typically put forward by various authors to explain the NM piezoresistive effect. Huang *et al.*[17] and Flandin *et al.*[21] report NM piezoresistance in the ethylene–octene elastomers filled with high-structure CB.

Bokobza and Belin[24] found decrease of resistivity versus strain on repeated stretching of the styrene–butadiene rubber filled with multiwalled carbon nanotubes (MWCNTs). Yamaguchi *et al.*[22] observed NM piezoresistance in the natural rubber and styrene butadiene rubber filled with N330 CB. Jha *et al.*[16] found surprisingly contrasting behavior of low- and high-structure CB fillers in natural rubber. Namely, high-structure CB showed reversible and monotonic (M) increase of resistance versus elongation, whereas low-structure N330 CB showed NM and irreversible piezoresistive behavior. Bloor *et al.*[19] observed strong negative piezoresistance for a silicone/urethane proprietary elastomer filled with nickel nanoparticles. Piece and Mitchell[23] observed strong negative piezoresistivity for polydimethylsiloxane filled with highly structured dendritic nickel nanoparticles. It seems reasonable from the above that the shape of the conducting particulates, the details of the interaction between the conductive filler and the insulator matrix, and thus, resulting morphology of the conducting network, all play crucial roles in determining a kind of piezoresistive response, but further clarification is strongly needed. In particular, it is desirable to study more systems with different elastomer matrices and fillers.

For this purpose, in the present work, eight different elastomeric materials were combined with MWCNTs, CB and nanoclay and sprayed onto vulcanized butyl rubber sheets. Additionally, the samples were crosslinked to improve mechanical and electrical properties and stretched repeatedly in one dimension with extensions of 50–150%. Two distinct piezoresistive behaviors were observed during these studies. In the first case, both the resistance and resistivity were found to monotonically grow with elongation. In the second case, however, the resistance and resistivity were found to decrease with elongation after an initial period of growth. The former was observed in nitrile- and styrene-containing elastomers, whereas the latter in chemically simpler (poly-)isoprene, butadiene, and isobutylene rubbers. The possibility to modify the piezoresistive behavior of the conductive elastomers (in particular toward an NM one) via chemical modification of the polymeric matrix opens up new venues for applications. Why NM piezoresistive effect could be important? Note that an NM or strongly nonlinear response of the system to an external perturbation (strain in our case) is paradigmatic to the dynamical systems exhibiting very complex kinds of nonlinear dynamics: bistability, periodic oscillations, even chaotic behavior.[26] Thus, the third class of stretchable conductors with NM response can be potentially used to construct a wide variety of novel complex devices (bistable elements, electromechanical oscillators, etc.), where NM change of resistance could be exploited to provide such an advanced functionality.

EXPERIMENTAL

Materials and Equipment

A total of eight different elastomers were studied. Polyisoprene (PIP) pellets (99+%. trans-1,4) and polystyrene-block-polyisoprene-block-polystyrene (PS-PI-PS) copolymer (styrene 22 wt %) were purchased from Sigma Aldrich and used as received. The following polymers were provided by LANXESS: butyl RB 100, butyl 402, Buna CB 23 (polybutadiene), Buna VSL 5025-2 HM (styrene–butadiene block copolymer), Krynac 3370 F (nitrile–butadiene copolymer), Therban® AT 3443 VP (hydrogenated nitrile–butadiene copolymer). Sheets of cured black butyl rubber approximately 500 μm thick were also obtained from LANXESS. HPLC grade chloroform was purchased from Fisher Scientific and used as received. MWCNTs with a diameter ranging from 5 to 15 μm and a length of approximately 50 μm were purchased from US Research Nanomaterials. CB Vulcan XC 72 (CB) was provided by LANXESS. Nanoclay (CL), Nanomer I.128E montmorillonite clay, surface modified with 25–30 wt % trimethyl stearyl ammonium was purchased from Aldrich.

SEM images of the coatings were taken using a Hitachi S-4500 field-emission scanning electron microscope. The solutions were ultrasonicated using a Bransonic 2510 bath sonicator at a frequency of 40 kHz and with an output power of 100 W.

A Badger 350 airbrush with a "heavy" nozzle was used for spraying of the dispersion/solutions. Pressurized (60 psi) ultrahigh purity nitrogen gas was used to feed the airbrush. The nozzle was kept at a distance of approximately 20 cm from the surface of the substrate.

Mitutoyo thickness gauges at LANXESS and Surface Science Western (SSW) were used to measure the thickness of the composite coatings. A Keithley 6517A electrometer and Keithley 2400 sourcemeter were used to measure sample resistance in either source–voltage or source–current regime, whichever was more appropriate.

Sample Preparation

The following procedure was used to prepare conductive coatings for all polymeric compounds containing 14% MWCNTs. A total of 35 mg of MWCNTs were dispersed in 245 mL of chloroform and ultrasonicated for 2 h. Next, 210 mg of *trans*-PIP was added to the solution, thus bringing the total concentration of solute to 1 mg/mL. The MWCNT/polymer blend was then sonicated for another 4 hours while maintaining the solution at a constant temperature. The solution was then sprayed onto a 3×8 cm^2 rectangular sheet of vulcanized black-filled butyl rubber. Spraying 245 mL of the solution took approximately 30 min, and it was imperative to keep the coating dry during this process. The samples were then left to dry for 24 h.

Samples containing either CB or nanoclay in addition to the MWCNTs were prepared using the same procedure. However, a total of 35 mg of either CB or CL were added to 245 mL of chloroform in the first stage together with the CNTs, and the rest of the preparation was identical to the one described above.

The thickness of the coating was measured as the difference in thickness before and after spraying (dry and crosslinked samples) and calculated as an arithmetic average of 6–9 measurements taken at different locations on a sample.

The dry coatings were cured using a Hyperthermal Hydrogen Induced Cross-linking technique (HHIC).[27–31] HHIC is a dry and chemical-free process using minute amount of molecular hydrogen gas to generate carbon radicals on the surface, which subsequently diffuse into the bulk and recombine, thus producing the intermolecular crosslinks. The HHIC reaction was carried out under the following conditions. An operating pressure of neutral hydrogen was maintained at 0.8 mTorr. Hydrogen

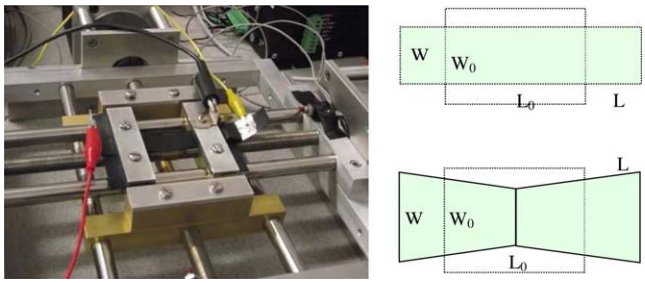

Figure 1. Left pane: image of the automated stretcher/IV measurement station showing sample mounting and lead connection. Right pane: shapes of ideal uniaxially stretched sample (top) versus a simplified real sample (bottom), where the sample is clamped at both ends during stretching. The unstretched samples are shown with dashed lines. [Color figure can be viewed in the online issue, which is available at wileyonlinelibrary.com.]

ions produced by electron–cyclotron–resonant plasma were extracted by an applied potential difference of −100 V at an extraction current of 10 mA into an electric field-free region where they were left to collide with background gas hydrogen molecules to generate hyperthermal neutral projectiles driving the crosslinking reaction. Above a sample holder, the remaining charged particles were reflected by an applied bias of 100 V (positive ions) and −50 V (electrons). The samples were cross-linked for 2 min.

Electrical Measurements

Following sample preparation, 2-probe *IV* (current–voltage) measurements were undertaken to obtain the resistance R of the samples. The *IV* curves were observed to be linear and symmetric around zero within the wide intervals of voltages and currents (e.g., −10 to +10 V, and 10^{-2} to 10^{-8} A). The (linear) resistance was thus well defined (at all sample elongations), and it was calculated according to the Ohm's Law as $R=V/I$, where V and I are either sourced or measured voltage and current.

To obtain sample resistance as a function of sample elongation, samples were mounted onto an automated stretcher shown in Figure 1 and simultaneously stretched and measured. Samples were stretched in one dimension at a constant speed of 0.3 mm/s up to 50% of their original length. Note that some samples were stretched up to 150%. The maximum applied elongation where the samples exhibited open circuit resistance was dependent upon the particular composite material, but it was always more than 50%.

In a source-voltage regime, a potential difference of 1 or 10 V was applied across the electrodes and the resulting current was measured. In a source-current regime, a constant current of 1×10^{-5} to 1×10^{-8} A was maintained during the measurement of the voltage (not exceeding a maximum of 1 V drop across the specimen).

Each sample was stretched 3–10 times leaving a day between consecutive measurements to allow the sample to relax. As butyl rubber is known for its superb elastic properties, the samples were observed to fully recover to their original dimensions after each stretching cycle.

Determination of Sheet Resistance and Bulk Resistivity of Samples

A few related physical quantities versus strain are reported in the literature for the piezoresistive effect. Care should be taken when comparisons are made for a variety of experimental situations, such as bulk samples, thin films, or films deposited on substrates. Authors interested in materials used for strain sensors, usually report their measurements in terms of raw resistance R of a sample or relative resistance change $(R-R_0)/R_0$, where the naught subscript represents the corresponding unstretched resistance. Those authors focused on the material properties of conductive composites, report their data in terms of bulk resistivity or conductivity $\rho=1/\sigma$. Other authors, studying thin conductive films, often present their data using sheet resistance defined as $R_{sq}=R\frac{W}{L}$, where W is the sample width, which equals the resistance of a square of arbitrary size cut from a conductive film. Knowing the thickness t of such a film, one can obtain the bulk resistivity via $\rho=R_{sq}t$. Since all three dimensions of the typically rectangular parallelepiped samples, L, W, and t, change, during deformation, one can encounter a situation where R is monotonically increasing, whereas ρ is decreasing with strain,[32] which might be potentially confusing over the details of the piezoresistive effect.

Moreover, samples often change their shape during stretching in an undesirable or uncontrollable way. For example, in our one-dimensional stretching tests, initially rectangular in-plane samples of dimensions $W_0 \times L_0$ change their shape to a "bow-tie," due to the clamping that constrains the unstretched sample width W_0 at both ends (Figure 1, right pane). Therefore, for the calculation of the sheet resistance, we take an average sample width $\langle W\rangle=\frac{W_0+W}{2}$, assuming piecewise-linear sample sides as sketched in the Figure 1, right pane, although the actual sample boundaries are curved. Furthermore, taking into account, the thickness ratio of the substrate and the conductive overlayer of ~10:1, we assumed that the change in width would be largely dominated by the properties of the substrate material. To confirm this assumption, we measured physical dimensions of unstretched and stretched samples using a vernier caliper. As an overlayer composite material we chose PIP as the most plastic polymer in the group and Therban® as the most elastic. The results are tabulated below.

Although the conductive film occupies only a ~1/10th of the overall sample thickness, it is enough to somewhat lower the Poisson's ratio for the case of PIP polymer matrix, as shown in Table I. This fact attests the noticeable coupling between strains/stresses in the substrate and the overlayer.

Table I. Poisson's Ratio for MWCNT/PIP and MWCNT/Therban® Composites on Butyl Rubber Substrate

Sample	Poisson's ratio
MWCNT/PIP	0.38 ± 0.02
MWCNT/Therban®	0.46 ± 0.03
Pristine butyl rubber	0.50 ± 0.00

Table II. Properties of the Studied 14% MWCNT/Polymer Blends on Vulcanized Butyl Rubber

Polymer	Polymer composition details	Average thickness (μm)	Piezoresistive behavior
Krynac 3370 F	33% acrylonitrile	33	M
Therban® AT 3443 VP	hydrogenated 34% acrylonitrile	40	M
Buna VSL 5025-2 HM (SBR)	25% styrene	54	M
PS-PI-PS	22% styrene	30	M (transitional to NM)
Buna CB 23	96% *cis*−1,4-polybutadiene	38	NM
butyl RB 100	1% PIP	30	NM
butyl 402	2% PIP	36	NM
trans-PIP	100% PIP	40	NM

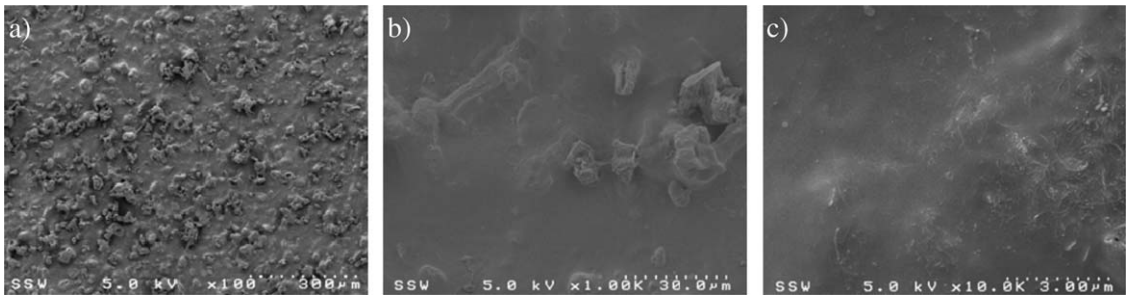

Figure 2. SEM images of an unstretched 14% MWCNT/PIP composite on butyl rubber at various magnifications.

In contrast, we cannot estimate the change of the thickness of the conductive film t during stretching. Therefore, we take $t=t_0$, $L=L_0(1+\varepsilon)$, $W=W_0(1+\varepsilon)^{-\nu}$, where $\varepsilon=(L-L_0)/L_0$ is the strain, the Poisson's ratio was taken as $\nu=0.4$ for PIP composites, while the quasi-universal value $\nu=0.5$ was used for all other materials including butyl rubber. This yields the following approximate formula for the sheet resistance:

$$R_{sq}=R\frac{\langle W\rangle}{L}=R\frac{W_0}{L_0}\frac{(1+\varepsilon)^{-\nu}+1}{2(1+\varepsilon)} \quad (1)$$

While, in principle, we can further correct this formula for the change of the conductive layer thickness, in the current form it corresponds to our best estimate of the sheet resistance based on the available experimental data. It needs to be emphasized that introducing a thickness correction into the formula for the sheet resistance would only amplify the observed NM features. In fact, we observe these NM features not only for the $R_{sq}(\varepsilon)$ curves, but even for the raw $R(\varepsilon)$ resistance versus strain dependences as obtained from the electrical measurements. This last fact may be important in the context of designing future engineering devices, which would exploit the nonmonotonicity in the piezoresistive effect.

RESULTS

After collecting the resistance data for all eight polymer/MWCNT composites, we observed two distinct piezoresistive behaviors. We refer to them as M and NM. In the first case, the resistance (sheet resistance) gradually increases with the applied strain until it reaches a point of virtual open circuit. The second case is markedly different. After an initial increase, the resistance (and sheet resistance) starts to decrease until it reaches a local minimum, after which it follows the same behavior as in the case one (Table II).

Note that all of the studied composites exhibited the same M piezoresistivity during the first stretch. The NM behavior arose upon the second and all subsequent stretches in the samples

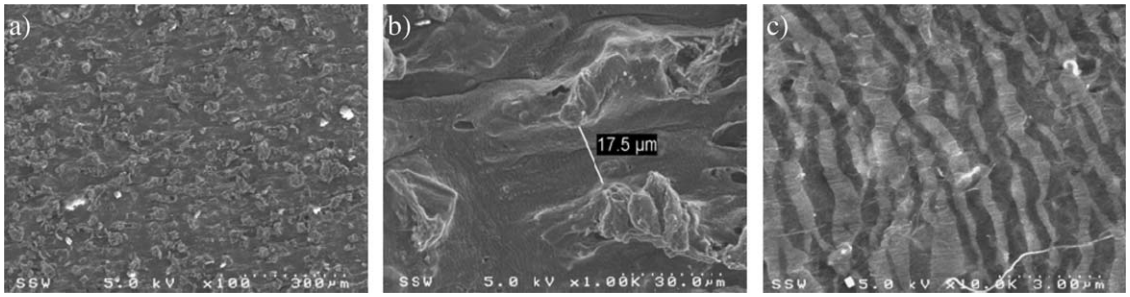

Figure 3. SEM images of a stretched (50% elongation) 14% MWCNT/PIP composite on butyl rubber at various magnifications. The direction of stretching is perpendicular to the "zebra" pattern.

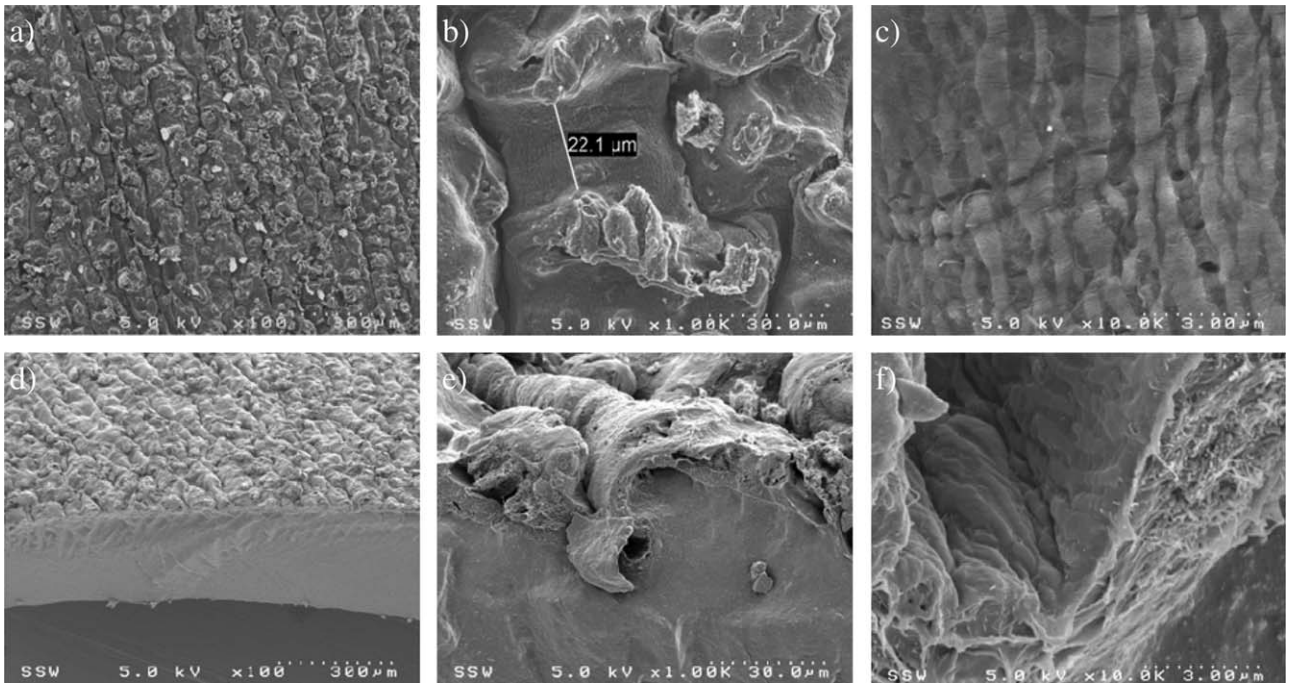

Figure 4. SEM images of a 14% MWCNT/PIP composite which was repeatedly stretched (50% elongation) and released to its original length. The direction of stretching is perpendicular to the zebra pattern. Shown are a top view (a–c) and a cross-sectional view after a freeze-fracture (d–f).

that exhibited it. We provide more details for these two classes of piezoresistive behavior below.

MWCNT/PIP Composites

PIP was selected as the matrix material for its great cross-linking properties using hyperthermal protons, as first observed by Zheng *et al.*[29] Probably due to a high concentration of unsaturated bonds, our MWCNT/PIP composites showed the highest degree of cross-linking using HHIC. Based on a series of independent tests measuring the depth of crosslinking using AFM (Young's modulus) and wash testing, it was estimated that an MWCNT/PIP blend crosslinks at a rate of ~1–2 μm/min.[33] It needs to be pointed out that given the exposure time of 2 min, only a few microns of the material could be effectively cross-linked depth wise. At same time, the average thickness of deposited coatings was measured to be ~40 μm (Table II). However, this thickness was largely determined by the size of the MWCNT bundles, while the conductive layer between the bundles was much thinner (few microns), as illustrated below.

Topographical images of the MWCNT/PIP composites as studied by SEM at different magnifications are shown in Figures 2–4. The most noticeable inhomogeneity observed were CNT bundles tens of microns in size. In general, the composite material consists of a uniform blend of PIP with well-dispersed CNTs. The composite layers also showed some porosity (see Figure 4), which is most likely due to bubbles trapped during spraying. Unlike the other MWCNT/rubber composites covered in the next section, the MWCNT/PIP composite films exhibited plasticity with irreversible deformation

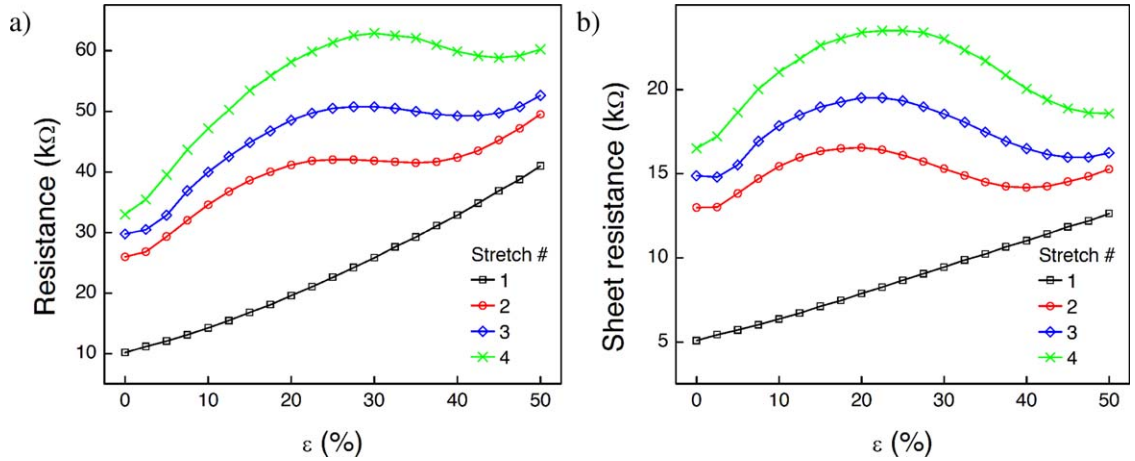

Figure 5. Overall sample resistance R, and sheet resistance R_{sq} as a function of strain ε for the MWCNT/PIP composites on butyl rubber substrate over four stretching cycles. [Color figure can be viewed in the online issue, which is available at wileyonlinelibrary.com.]

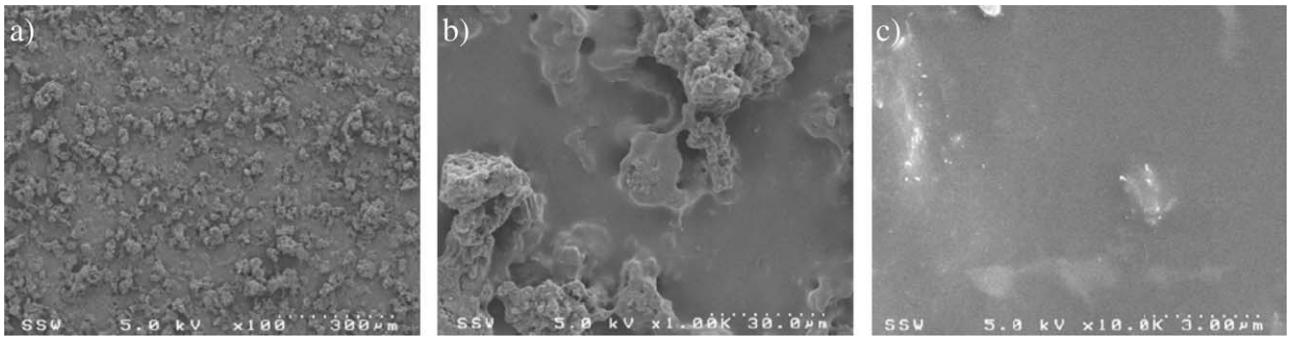

Figure 6. SEM images of a 14% MWCNT/Therban® composite on butyl rubber at various magnifications.

upon the first stretch, resulting in the formation of a buckled layer after subsequent release of the strain (see Figure 4).

For 14% MWCNT/PIP samples, both the overall resistance $R(\varepsilon)$ and the sheet resistance $R_{sq}(\varepsilon)$ [calculated according to eq. (2)] were found to behave nonmonotonically with strain ε during repetitive stretching (see Figure 5). For all PIP samples with a 14% MWCNT loading, the maximum value of the sheet resistance was found at approximately 25% elongation.

Other MWCNT/Elastomer Composites

The other seven MWCNT/elastomer composites on vulcanized butyl rubber, including Krynac, Therban®, Buna VSL, Buna CB, Butyl RB 100, Butyl 402, and PI-PS-PI, were mixed at 14% CNT loading and stretched to 50% elongation. In all these elastomers, no plasticity was visible by SEM upon stretching (at least up to 50%), as illustrated in Figures 6 and 7 for the MWCNT/Therban® blend. The first three elastomers exhibited an overall M piezoresistive behavior (see Figure 8), whereas the next three followed the same NM behavior as observed in MWCNT/PIP blends (Figure 9). The PI-PS-PI sample showed a transitional NM piezoresistance, where the maximum of sheet resistance was poorly developed (see Figure 10). It should be noted that the maximum value of the sheet resistance in NM piezoresistive behavior was found at approximately 25% elongation for all those elastomer blends, where it was observed.

Data summarized in Table II suggest that the type of piezoresistive behavior is correlated to the percentage of the nitrile and/or styrene groups in the polymer. Polymers having the highest (~25% or more) nitrile or styrene content show monotonic piezoresistive behavior, while those having no or few styrene or nitrile groups show NM piezoresistive behavior and the PI-PS-PI with 22% styrene lies in between). Although we presently do not know the mechanism (either direct or indirect) responsible for such correlation, it deserves further attention.

Influence of the Second Filler in the Ternary Composites

The correlation between the chemical nature of the polymer matrix and the character of piezoresistive behavior in a composite revealed in the previous section suggests that the atomic-scale details of the interaction of the polymer with the CNTs might be responsible for it. In an attempt to modify such interaction between the polymer and the CNTs, we prepared ternary mixtures by adding a third constituent. For this purpose, we selected both conductive and nonconductive nanoparticles. The conductive nanoparticles were chosen to be CB, while organo-nanoclay (CL) served as the nonconductive constituent, which, according to the literature, enhances the dispersion of CNTs in a polymer matrix.[34] We prepared and stretched these ternary composite samples in the same way as was described before for the binary compounds. The results are summarized in Figure 11.

When adding CB or organo-nanoclay to the composites we chose to keep the same amount of CNTs in the ternary mixtures as in the binary mixtures (35 mg of MWCNT per 210 mg of polymer) to preserve the original ratio of CNT to polymer. The third component, equal in mass to the MWCNT, was regarded merely as a modifier of the effective interaction between the CNTs and the polymer. The sheet resistance graphs shown in Figure 11(a) demonstrate that, as a conductive

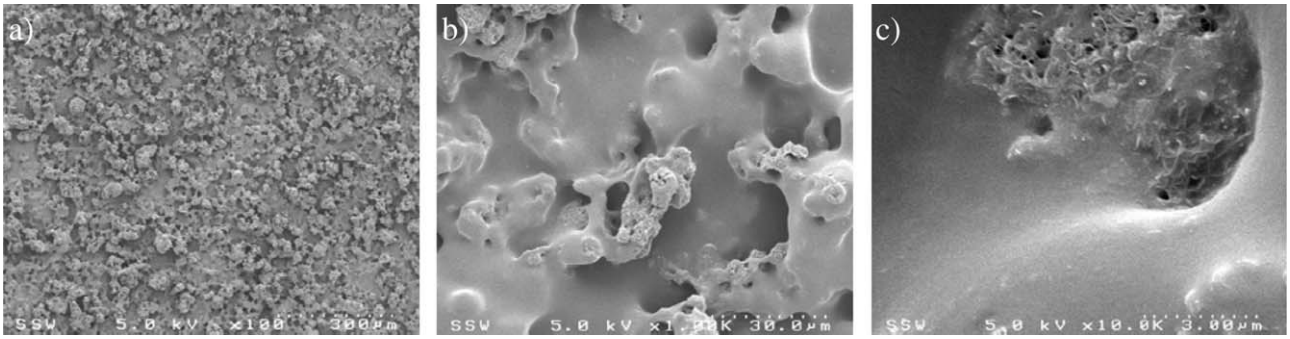

Figure 7. SEM images of a repetitively stretched/released 14% MWCNT/Therban® composite on butyl rubber at various magnifications. No changes in the morphology were observed.

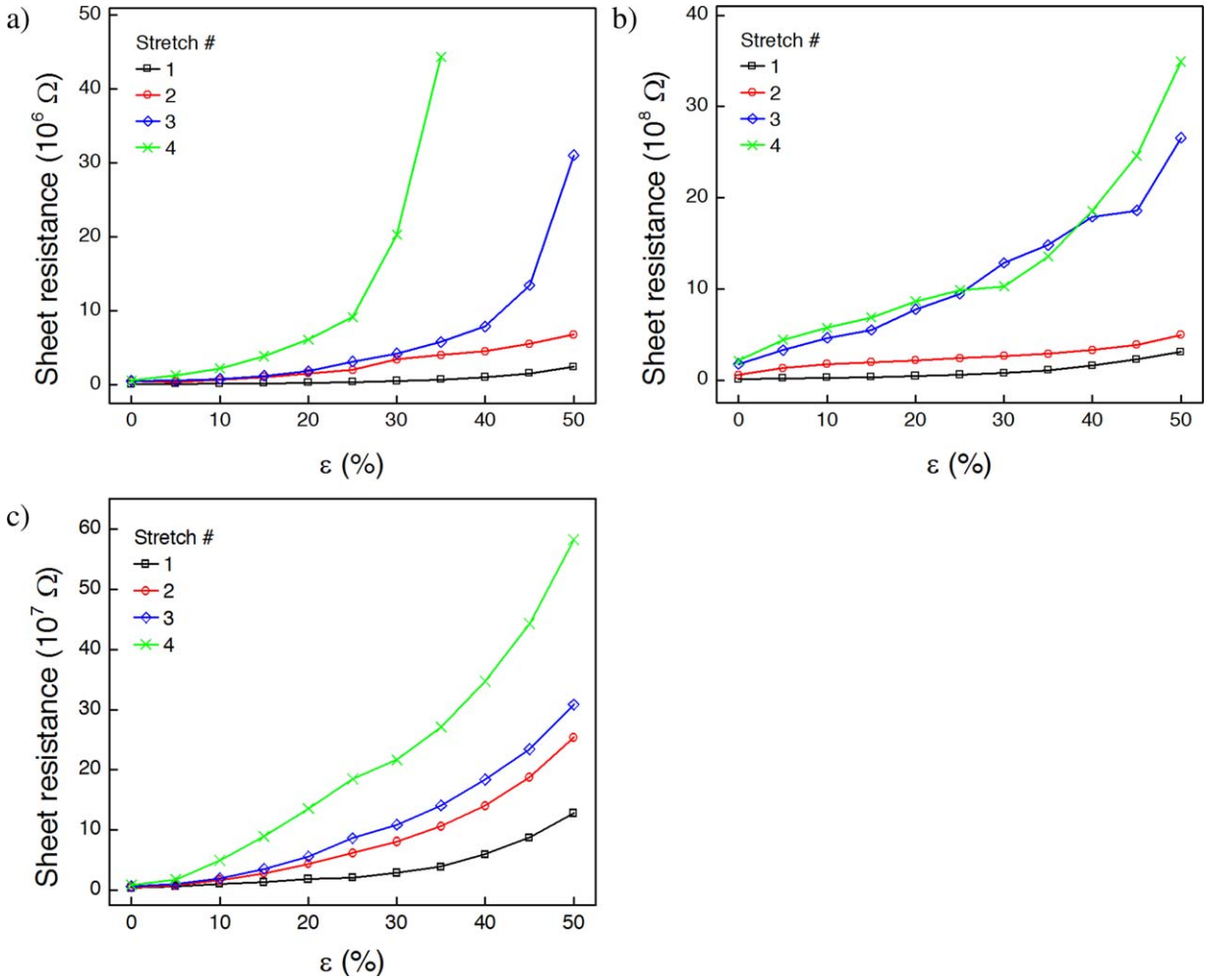

Figure 8. Sheet resistance curves as a function of applied strain for a 14% MWCNT/elastomer blend on butyl rubber with 50% maximum elongation: (a) Krynac 3370 F, (b) Therban® AT 3443 VP, and (c) Buna VSL 5025-2 HM. [Color figure can be viewed in the online issue, which is available at wileyonlinelibrary.com.]

substance, CB improved the overall conductive properties of the film by an order of magnitude. Moreover, it also preserved the NM piezoresistive behavior, while shifting the sheet resistance maximum toward lower strains (~15% elongation). Organo-nanoclay also improved the overall conductive properties of the composite film [~2 times, cf. Figures 11(b) and 5(b)] at zero strain. However, the slope of the $R_{sq}(\varepsilon)$ dependence on the first stretch was observed to be higher in the CL-containing samples compared to the original MWCNT/PIP blend, thus any increase in conductivity was lost at ~50% elongation. In addition, the organo-nanoclay seems to nearly destroy the NM piezoresistive behavior.

Dependence of Resistance on Crosslinking

To quantify the effect of crosslinking on piezoresistive response, we compared two composites selected from each piezoresistive group: (1) MWCNT/Therban® on butyl rubber exhibiting M behavior and (2) MWCNT/PIP on butyl rubber exhibiting NM behavior. We found that crosslinking does not affect the character of piezoresistive response of MWCNT/polymer composites. While it was impossible to carry out this experiment in a way where every sample would be first measured as pristine and subsequently crosslinked, we attempted to create almost identical samples. Although the samples were prepared at the same time under the same conditions, the measured absolute resistance values could differ up to two to three times for different samples.

However, the qualitative features of the piezoresistive curves were observed to be similar for identically prepared samples made of the same filler/matrix pair. Possible reasons for the variation of the absolute sheet resistance may include, (i) the surface roughness of the samples may vary, affecting the contact area between the sample and the electrodes and (ii) poorly controlled variables during manual spraying may affect the sample morphology (such variables as the distance from the nozzle to the sample, speed and character of nozzle motion over the sample surface, even the humidity of the environment, etc.). Nevertheless, the current set of data allows us to fully support our qualitative claims.

DISCUSSION

The findings described above raise a number of interesting questions. Firstly, what is the nature of the NM piezoresistive

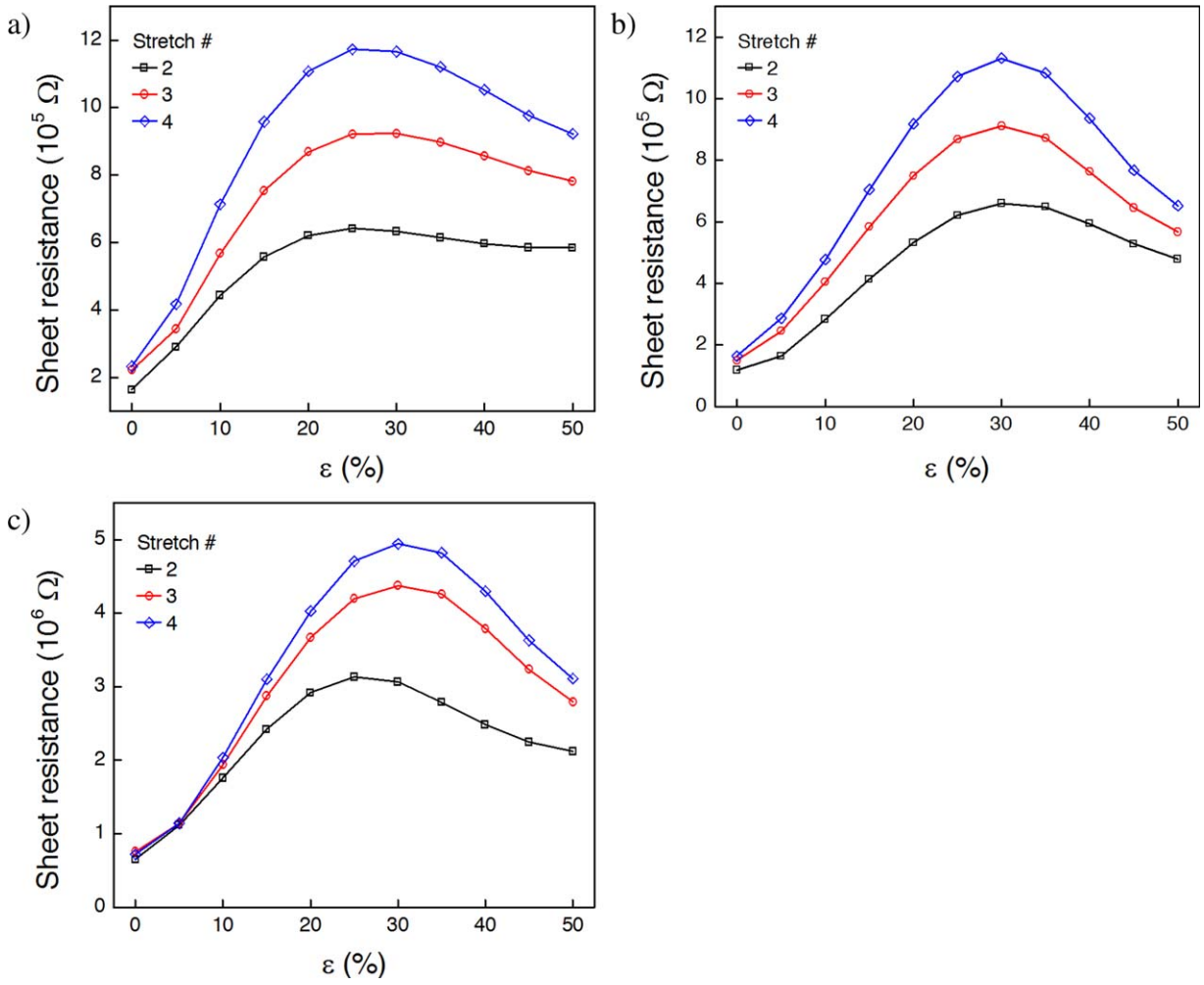

Figure 9. Sheet resistance curves as a function of applied strain for a 14% MWCNT/elastomer blend on butyl rubber substrate with 50% maximum elongation: (a) Buna CB 23, (b) butyl TP BTR RB 100, and (c) Butyl 402. [Color figure can be viewed in the online issue, which is available at wileyonlinelibrary.com.]

effect? As previously mentioned, M piezoresistive behavior is a generic scenario widely reported in the literature for simple conductors like metals as well as for more complex systems such as semiconductors, and also for the composite conductors such as CNT/polymer. In the case of metals, the explanation is trivial (as mentioned in the Introduction). For semiconductors, an "anomalous" decrease of the resistivity with elongation in silicon nanowires has been reported, and it was attributed to the drastic increase of the mobility of the charge carriers under strain.[2] One cannot exclude a similar effect operating in CNT as well, especially since CNT can be partially semiconductive. For the CNT/polymer systems, however, the conventional increase in resistance with tensile strain is usually attributed to the degradation of the conductive network via decreasing the number of contacts between CNTs.

On the other hand, NM piezoresistive behavior is more complicated as it involves competing effects, resulting in a decrease in resistance/resistivity of a stretched sample in a particular range of elongations only. This means that some yet unknown mechanism is responsible for the increase of net charge transport/number of contacts between CNTs. So far, there have only been a few observations in the literature of a decrease in resistivity with elongation for conductive polymer composites,[16–24] although none of them clearly report the decrease of the overall sample resistance with elongation the same way as reported here [see Figure 5(a)]. The systems studied in the literature included both elastomeric and nonelastomeric composites with such conductive fillers as CNTs, CB, and metallic nanoparticles. No comprehensive explanation of this phenomenon has yet been provided, although authors typically try to exploit the idea of increasing number of contacts between the conductive inclusions induced by uniaxial stretching of the sample (and the resulting contraction in the transverse direction).

One should emphasize that the samples we prepared and analyzed differ in one subtle but important aspect from most of the systems studied in the literature. Our system consists of a relatively thin (~40 microns or less) conductive overlayer sprayed on top of a relatively thick (~500 μm) vulcanized butyl rubber substrate as opposed to typically bulk samples or self-standing films. Thus, the stretching apparatus and the elastic properties of the butyl

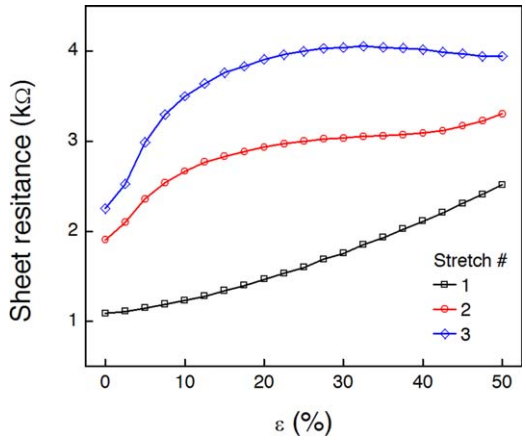

Figure 10. Sheet resistance curves as a function of applied strain for a 14% MWCNT/elastomer blend on butyl rubber with 50% maximum elongation for PI-PS-PI. [Color figure can be viewed in the online issue, which is available at wileyonlinelibrary.com.]

substrate, namely its Poisson's ratio $\nu \approx 0.5$, completely dominate (or strongly affect, in the case of PIP overlayer which shows $\nu \approx 0.4$, Table I) the lateral strain of the conductive layer. The only dimension where the elastic response is self-controlled by the overlayer is its thickness, which we cannot reliably measure during stretching.

For example, Figures 3(b) and 4(b) show the same spot on the surface of an MWCNT/PIP sample in two states: stretched (ε=50%) and released after stretch, respectively. In both images, one can clearly identify two particular CNT bundles with a "channel" of a uniform MWCNT/PIP conductive mixture in between. The width of this channels is W=17.5 μm when stretched and W_0=22.1 μm when released, and the ratio is $W/W_0 \approx 0.79$. This ratio is very close to the one obtained from the formula $W=W_0(1+\varepsilon)^{-\nu}$, where ν=0.5 for butyl rubber, $W/W_0 \approx 0.82$. In fact, the calculated ratio 0.79 is less than 0.82 for pure butyl rubber because the CNT bundles are rigid and so all the strain applied to the sample is accommodated in the "channels" between the CNT bundles. This circumstance might be important in the context of the observed NM piezoresistive effect, where such a strong local contraction in the direction perpendicular to stretching is likely responsible for bringing more nanotubes in the "channel" closer together thus enhancing formation of the new conductive paths, and effectively decreasing sample resistance. This simple analysis suggests that the multilayer nature of our samples (thin overlayer on top of a thicker substrate) might enhance the NM piezoresistive behavior.

Secondly, one should wonder what is the mechanism responsible for the qualitative difference in the conductive properties of the composite samples (NM vs. M piezoresistive effect) when the polymer matrix is changed? While we do not know the exact answer to this question yet, the current work presents a set of data, clearly showing the existence of the phenomenon itself as well as its various aspects. Moreover, our current results suggest that the increasing amount of nitrile and/or styrene groups in the polymer matrix changes the piezoresistive behavior in the composite from NM to M. Let us note here, that the carbon rings in nanotubes and CB should have a relatively strong attractive π-stacking interaction with styrene functional groups in the polymer matrix. One should also consider in this context possible steric effects of the styrene and nitrile side groups, which would affect the wrapping of the polymer chains around the nanotubes. One may speculate, thus, that presence of the styrene/nitrile groups in the polymer matrix effectively prevents easy formation of the new contacts between conductive fillers upon stretching of the sample, and/or allows for easy breaking of the existing contacts between the filler particles.

Thirdly, similar argumentation can also help to explain the shift of the resistance maximum towards higher strains and eventual disappearance of the NM piezoresistive effect in the case of addition of nonconductive organo-clay to our CNT/PIP mixtures [cf. Figures 5(b) and 11(b)]. Indeed, as the organo-clay effective improves CNT dispersion, it also screens individual CNT from easily contacting each other upon stretching of the

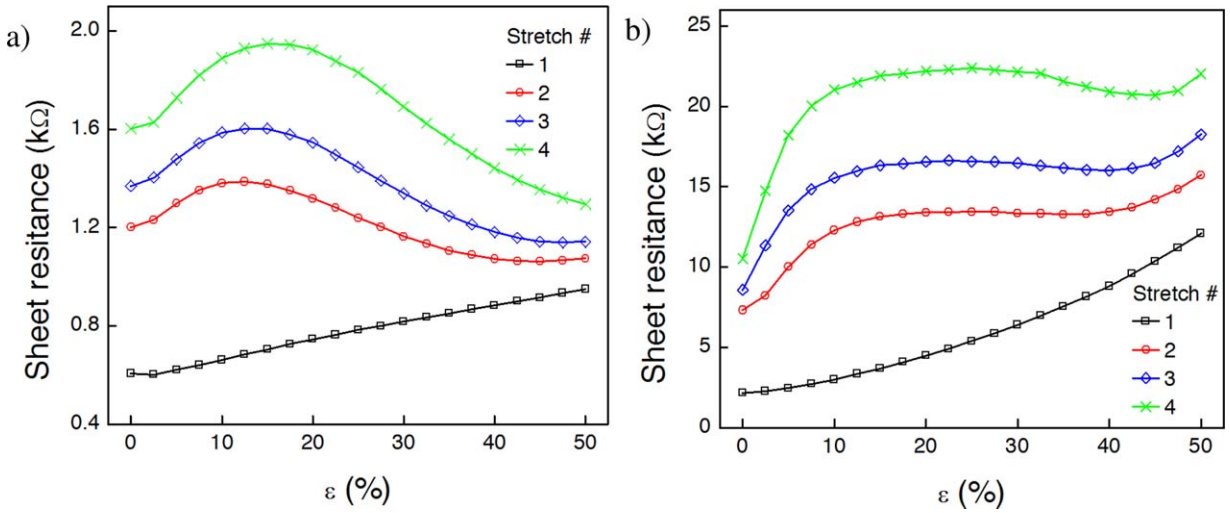

Figure 11. Sheet resistance curves as a function of applied strain for samples made of ternary mixtures [cf. Figure 5(b)]: (a) (12.5% MWCNT + 12.5% CB)/PIP; (b) (12.5% MWCNT + 12.5% CL)/PIP. [Color figure can be viewed in the online issue, which is available at wileyonlinelibrary.com.]

sample. It should be noted that addition of secondary nanofiller to tune piezoresistive effect in the nanocomposite samples has been recently explored by Bilotti *et al.*[35]

Fourthly, as it has been already mentioned in the Introduction section, the NM piezoresistive response of the systems studied in the present work may open ways for novel application of stretchable conductors. Namely, no-monotonic response of the system to an external perturbation is a paradigmatic concept in the studies of nonlinear dynamical systems that can exhibit very complex behaviors, such as bi- or multistability, periodic oscillations, deterministic chaos, and so forth.[26] A famous but relatively simple example of such a system is the logistic map.[36] In our context, one can propose, for example, to couple the NM response of our system $R(\varepsilon)$ to the apparatus proving the stretching (ε) itself, via a feedback loop. While practical implementations and details of such setup may vary, it is obvious that in this way one may replicate many salient features of a complex nonlinear dynamical system: fixed points, periodic attractors, period-doubling bifurcations, chaotic regime. These nonlinear dynamical features may be utilized to build, for example, electromechanical switches, oscillators, and so forth, and other advanced functionalities beyond simple pressure/strain sensing.

CONCLUSIONS

In summary, even if a full explanation of the observed NM piezoresistive effect is still desired, based on the obtained data, we can draw the following conclusions. Depending on the chemical nature of the insulating polymer matrix of the MWCNT/polymer composite conductive samples, we observed two distinct piezoresistive behaviors being M and NM. Current results suggest that the increasing amount of nitrile and/or styrene side groups in the polymer matrix changes the piezoresistive effect in the composite from NM to M. Namely, the polymers having the highest (~25%wt or more) nitrile or styrene content clearly show M peizoresistive behavior, while those having no or few styrene or nitrile groups show NM piezoresistive behavior. The direct or indirect mechanism giving rise to such a correlation will be further investigated.

It was also observed that adding an isotropic conductor (CB) to the composite film results in a shift of the sheet resistance maximum toward lower strains. The addition of nonconductive nanoparticles (organo-clay) to the composite seems to stifle the NM piezoresistive behavior. While the organo-clay improves the overall conductivity in the unstretched samples, it also increases the slope of resistance versus strain, which is of great interest to the designers of strain sensors.

Finally, we propose that the novel stretchable conductors with an NM response open a new venue for advanced applications and complex functionalities inspired by paradigmatic examples in the nonlinear dynamical systems, namely bi- or multistability, periodic oscillations, bifurcations, chaotic behavior, and so forth, which enables one to construct advanced micro-electro-mechanical machinery.

ACKNOWLEDGMENTS

The authors are grateful for the financial support from LANXESS Inc., Ontario Research Fund (ORF), Natural Science and Engineering Research Council of Canada (NSERC), and Canada Foundation for Innovation (CFI).

REFERENCES

1. Barlian, A. A.; Park, W. T.; Mallon, J. R.; Rastegar, A. J.; Pruitt, B. L. *Proc. IEEE* **2009**, *97*, 513.
2. Lugstein, A.; Steinmair, M.; Steiger, A.; Kosina, H.; Bertagnolli, E. *Nano Lett.* **2010**, *10*, 3204.
3. Park, J.; You, I.; Shin, S.; Jeong, U. *ChemPhysChem* **2015**, *16*, 1155.
4. Bokobza, L. *Polymer* **2007**, *48*, 4907.
5. Ponnamma, D.; Sadasivuni, K. K.; Grohens, Y.; Guo, Q.; Thomas, S. *J. Mater. Chem. C* **2014**, *2*, 8446.
6. Kane, C. L.; Mele, E. J. *Phys. Rev. Lett.* **1997**, *78*, 1932.
7. Nardelli, M. B.; Bernholc, J. *Phys. Rev. B* **1999**, *60*, R16338.
8. Rochefort, A.; Salahub, D. R.; Avouris, P. *Chem. Phys. Lett.* **1998**, *297*(1–2), 45.
9. Tombler, T. W.; Zhou, C. W.; Alexseyev, L.; Kong, J.; Dai, H. J.; Liu, L.; Jayanthi, C. S.; Tang, M.; Wu, S.-Y. *Nature* **2000**, *405*, 769.
10. Knite, M.; Tupureina, V.; Fuith, A.; Zavickis, J.; Teteris, V. *Mater. Sci. Eng. C* **2007**, *27*, 1125.
11. Chun, K.-Y.; Oh, Y.; Rho, J.; Ahn, J.-H.; Kim, Y.-J.; Choi, H. R.; Baik, S. *Nat. Nano* **2010**, *5*, 853.
12. Park, M.; Kim, H.; Youngblood, J. P. *Nanotechnology* **2008**, *19*, 055705.
13. Wichmann, M. H. G.; Buschhorn, S. T.; Gehrmann, J.; Schulte, K. *Phys. Rev. B* **2009**, *80*, 245437.
14. Oliva-Aviles, A. I.; Aviles, F.; Sosa, V. *Carbon* **2011**, *49*, 2989.
15. Lipomi, D. J.; Vosgueritchian, M.; Tee, B. C.-K.; Hellstrom, S. L.; Lee, J. A.; Fox, C. H.; Bao, Z. *Nature Nanotechnology* **2011**, *6*, 788–792.
16. Jha, V.; Thomas, A. G.; Bennett, M.; Busfield, J. J. C. *J. Appl. Polym. Sci.* **2010**, *116*, 541.
17. Huang, J.-C.; Huang, H.-L. *J. Polym. Eng.* **1997**, *17*, 213.
18. Wang, S.; Chung, D. D. L. *J. Mat. Sci.* **2007**, *42*, 4987.
19. Bloor, D.; Donnelly, K.; Hands, P. J.; Laughlin, P.; Lussey, D. *J. Phys. D: Appl. Phys.* **2005**, *38*, 2851.
20. Busfield, J. J. C.; Thomas, A. G.; Yamaguchi, K. *J. Polym. Sci. B: Polym. Phys.* **2004**, *42*, 2161.
21. Flandin, L.; Chang, A.; Nazarenko, S.; Hiltner, A.; Baer, E. *J. Appl. Polym. Sci.* **2000**, *76*, 894.
22. Yamaguchi, K.; Busfield, J. J. C.; Thomas, A. G. *J. Polym. Sci. B: Polym. Phys.* **2003**, *41*, 2079.
23. Peace, M. H. K.; Mitchell, G. R. *J. Phys. Conf. Ser.* **2009**, *183*, 012011.
24. Bokobza, L.; Belin, C. *J. Appl. Polym. Sci.* **2007**, *105*, 2054.

25. Ronald Hugh, N. Conductive Rubbers and Plastics: Their Production, Application and Test Methods; Elsevier Pub. Co.: Amsterdam, New York, **1970**.
26. Strogatz, S. H. Nonlinear Dynamics and Chaos: With Applications to Physics, Biology, Chemistry, and Engineering; Westview Press: Boulder, Colorado, **1994**.
27. Liu, Y.; Yang, D. Q.; Nie, H. Y.; Lau, W. M.; Yang, J. *J. Chem. Phys.* **2011**, *134*, 074704.
28. Zheng, Z.; Xu, X. D.; Fan, X. L.; Lau, W. M.; Kwok, R. W. M. *J. Am. Chem. Soc.* **2004**, *126*, 1233612342.
29. Zheng, Z.; Kwok, W. M.; Lau, W. M. *Chem. Commun.* **2006**, 3122.
30. Zheng, Z.; Wong, K. W.; Lau, W. C.; Kwok, R. W. M.; Lau, W. M. *Eur. J.* **2007**, *13*, 3187.
31. Trebicky, T.; Crewdson, P.; Paliy, M.; Bello, I.; Nie, H. Y.; Zheng, Z.; Fan, X. L.; Yang, J.; Gillies, E. R.; Tang, C.; Liu, H.; Wong, K. W.; Lau, W. M. *Green Chem.* **2014**, *16*, 1316–1325.
32. Yu, Z.; Niu, X.; Liu, Z.; Pei, Q. *Adv. Mater.* **2011**, *23*, 3989.
33. Guo, Q.; Paliy, M.; Kobe, B.; Trebicky, T.; Suhan, N.; Arsenault, G.; Ferrari, L.; Yang, J. *J. Appl. Polym. Sci.* **2015**, *132*, 41493, DOI: 10.1002/app.41493.
34. Levchenko, V.; Mamunya, Y.; Boiteux, G.; Lebovka, M.; Alcouffe, P.; Seytre, G.; Lebedev, E. *Eur. Polym. J.* **2011**, *47*, 1351.
35. Bilotti, E.; Zhang, H.; Deng, H.; Zhang, R.; Fu, Q.; Peijs, T. *Compos. Sci. Technol.* **2013**, *74*, 85.
36. May, R. M. *Nature* **1976**, *261*, 459.